The Serotonergic Neural Circuit Between The Dorsal Raphe Nucleus And The Basolateral Amygdala Is Implicated In Modulating The Arousal from Sevoflurane Anesthesia

Qian Yu[1], LeYuan Gu[1], XiTing Lian[2], YuLing Wang[1], Qing Xu[2], HaiXiang Ma[1], Lu Liu[2], WeiHui Shao, JiaXuan GU[1], Yue Shen[2], LiHai Chen[4], HongHai Zhang*[1,2,3]

[1]Department of Anesthesiology, the Fourth Clinical School of Medicine, Zhejiang Chinese Medical University, Hangzhou, 310006, China

[2]Department of Anesthesiology, Affiliated Hangzhou First People's Hospital, Zhejiang University School of Medicine, Hangzhou, 310006, China

[3]Westlake Laboratory of Life Sciences and Biomedicine, Hangzhou, 310006, China

[4]Department of anesthesiology，Nanjing First Hospital，Nanjing Medical University, NanJing, China

Qian Yu, LeYuan Gu, XiTing Lian, YuLing Wang, Qing Xu contributed equally to this work

Corresponding authors: HongHai Zhang

Email address: zhh0902@zju.edu.com

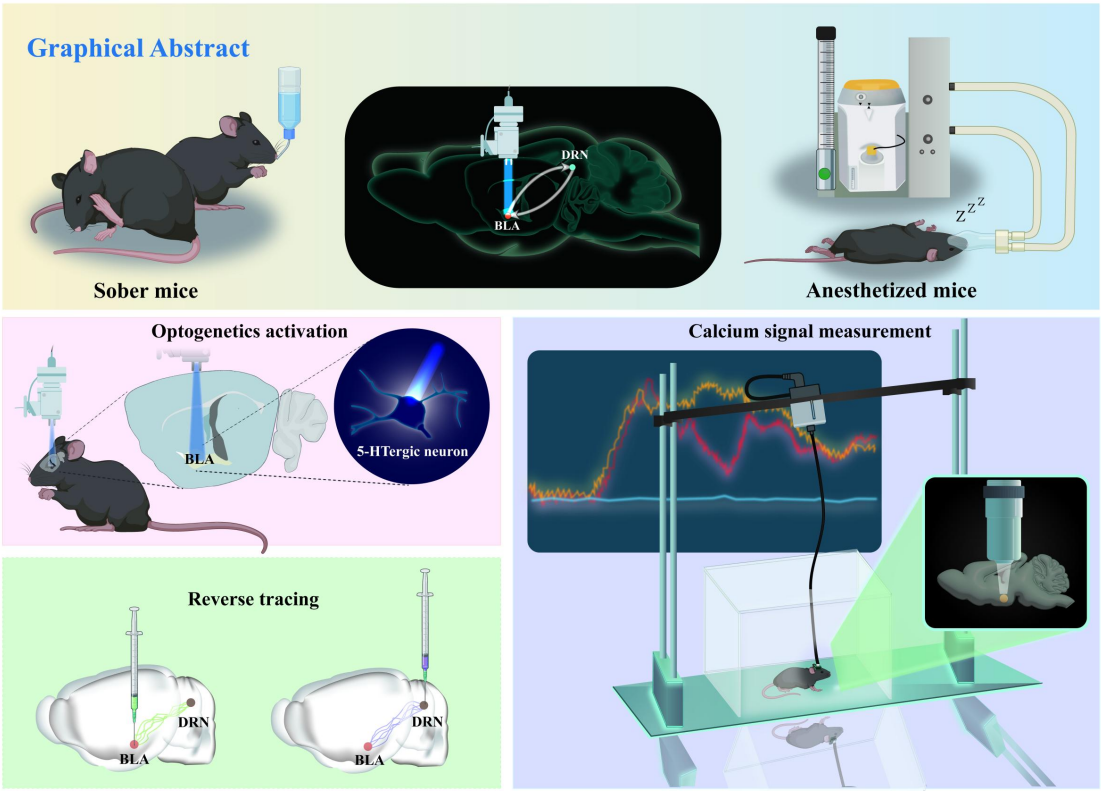

Abstract

Although some advancements concerning the arousal involved in mediating the delayed emergency from general anesthesia,which will lead to the serious complications, had been made, the role by arousal in modulating in delayed emergency still remains to be unclear. In our models, based on our previous working that activation of the 5-Hydroxytryptamine (5-HT) neurons in the dorsal raphe nucleus (DRN) by optogenetics can significantly reduce the emergency time by activating arousal pathway, we further test whether the serotonergic neural circuit between the DRN and the basolateral amygdala (BLA) is implicated in modulating the arousal from the sevoflurane anesthesia and the emergency time of sevoflurane anesthesia by the pharmacological , optogenetics and fiber photometry. Our findings showed that whether the serotonergic neural circuit between the DRN and the basolateral amygdala (BLA) plays a key role in modulating the arousal from the sevoflurane anesthesia and the emergency time of sevoflurane anesthesia. Based on the serotonergic neural circuit, the 5-HT 1 A receptor is of great significance to mediate the arousal and the emergency time of the sevoflurane anesthesia.

Introduction

General anesthesia, which can be described as a pharmacologically induced state of amnesia, immobility, unconsciousness, and analgesia, has been widely used in surgery for nearly two centuries because of its ability to induce reversible loss of consciousness and maintain physiological stability[1]. General anesthesia is a reversible coma rather than analogous to any phase of sleep[2]. Previous studies have shown that under general anesthesia, the brain remains responsive to somatosensory, auditory, and visual stimuli， instead of silent, or unresponsive to external stimuli[3, 4, 5]. Most studies on the mechanism of arousal from general anesthesia in the past few years have focused on describing the action of anesthetic drugs on molecular targets[6]. Recently, researchers have begun to describe how anesthetics acted on specific neural circuits to cause the changes in arousal [7, 8], and shown that anesthesia-induced loss of consciousness occured through specific interactions with neural circuits in the central nervous system that regulated the endogenous sleep-wake system, such as the

parbrachial nucleus, lateral hypothalamus, locus coeruleus, ventral tegmental area, ventrolateral preoptic nucleus[9, 10, 11, 12], and optogenetic techniques were used in most of the experiments. However, whether other critical arousal promoting regions and their neural circuits are involved in the regulation of consciousness under general anesthesia is still unknown.

The amygdala plays an important role in initiating appropriate neurobehavioral responses to emotionally arousing events and activation of amygdala could promote REM and related activity. The amygdala is classified into three areas, as the basolateral, cortical, and central nuclei, and the functions are heterogeneous [13]. Although many studies have not distinguished functional roles for nuclei of the amygdala, the available evidence suggests that the basolateral nucleus of the amygdala (BLA) is also involved in regulating REM and sends outputs to the central amygdala, sending neural information to the hypothalamus and the brainstem [14, 15]. In behavioral control over breathing, the limbic cortex, especially the amygdala, is a major regulator of the emotion-associated breathing[16].

It has been suggested that basal dopamine release from the BLA increases RR via local postsynaptic D2-like receptors, which might be related to the mechanisms of enhancement or inhibition of breathing[17]. It has been found that breathing and awakening are closely related. Just as sleep status can affect breathing control, changes in breathing can also lead to changes in wakefulness. Mice genetically deficient in serotonin neurons (Lmx1bf/f/p) in the central nervous system have been shown to have impaired arousal to CO_2, but display normal arousal to hypoxia, sound, and mechanical stimuli, suggesting that serotonin neurons were involved in CO_2 -induced sleep arousal[18]. 5-HT neurons, including midbrain neurons involved in sleep-wake regulation, respond to increased concentrations of inhaled CO_2, resulting in increased firing rates, which may occur through a mechanism mediated by the 5-HT receptor[19, 20, 21, 22]. The dorsal raphe nucleus (DR), as the main source of 5-HT innervation in the forebrain, is involved in a variety of functions including anxiety, depression, and sleep-wake cycles, especially increased respiration and arousal induced by elevated levels of CO_2[23]. The electrical activity of its serotonergic neurons

and the release of serotonin in the serotonergic projection area are increased during wakefulness and decreased during sleep. Furthermore, inactivation of the limbic structures that project to the hippocampus, such as pirifrom cortex, entorhinal cortex, or BLA, delay emergence from halothane and pentobarbital anesthesia and often reduced anesthetic-induced behavioral excitation[24, 25, 26]. Thus, we hypothesized a link between BLA and arousal from anesthesia and 5-HT in DR may also play a role in, but the precise neural mechanisms for this regulation, however, remain unclear.

Methods

2.1 Animals

The experimental animals in this study are all wild type C57BL/6J mice, purchased from the Animal Experiment Center of Zhejiang University, and the experimental protocol was approved by the Experimental Animal Ethics Committee of Zhejiang University. All mice were housed in the barrier breeding room (SPF level), with appropriate temperature and humidity, clean living environment, and free access to food and water. For the experiments, eight-week-old mice weighing 20-25g were chosen. In order to avoid the interference of the estrous cycle of female mice, only male mice were used for behavioral experiments, which were completed from 9:00 to 15:00.

2.2 Sevoflurane anesthesia modeling and method of anesthesia induction and emergency time observation

The 8-week-old C57BL/6J mice were placed in a well-airtight inhalation anesthesia box (size, model size: length: 20cm, width: 10cm, height: 15cm; Reward) for 30 minutes prior to the experiment to adapt to the experimental environment. After 30 minutes of adaptation, the gas concentration of the sevoflurane volatilization tank was adjusted, and the anesthesia box was rotated 90 degrees every 15 s. When the mouse was in an abnormal position and could not turn itself prone onto all four limbs, the loss of righting reflex (LORR) was recorded as the Induction Time, and LORR was marked as the beginning of anesthesia maintenance phase. The corresponding experimental operation was carried out during maintenance phase in accordance with the experimental design. The sevoflurane volatilization tank was closed at the 30th

minute of anesthesia to stop inhalation anesthesia, and the residual sevoflurane in the anesthesia box and pipeline was removed by rapid oxygenation, with the oxygen flow rate maintained at 2L/min. The anesthesia box was rotated 90 degrees every 15 s. The recovery of righting reflex (RORR) was considered if the mouse was in an abnormal position and could voluntarily place all four feet on the floor. The time between the end of anesthesia and RORR was recorded as the Emergency Time.

2.3 Stereotactic and virus microinjection surgery

8-week-old DBA/1 mice were anesthetized with 3.5% chloral hydrate and fixed in the head with a stereotactic apparatus (68018, RWD Life Sciences, Inc., Shenzhen, China). The body temperature of anesthetized mice were kept constant at 37°C during the procedure using a heating pad. For optogenetic viral delivery, pAAV-TPH2 PRO-ChETA-EYFP-WPRES-PAS (100nL, titer: 10^{13}vg/ml, Shanghai Shengbo Biotechnology Company) or rAAV-TPH2-GCaMP6S-WPRE-hGH pA (100nL, titer: 10^{12}vg/ml, Wuhan Zumi Brain Science and Technology Co., LTD.) was microinjected into unilateral or bilateral BLA (AP: -0.40mm; ML: + / - 2.95 mm; DV: -5.00 mm), based on mouse brain atlas (100nl, at a rate of 40 nl/min). Viruses were delivered via a gauge needle for the specification of 10ul controlled by an Ultra Micro Pump (160494 F10E, WPI). The syringe was not removed until 10 minutes after the end of the injection to allow the virus to spread. Then an optical fiber (FOC-W-1.25-200-0.37-3.0, Inper, Hangzhou, China) is implanted in the same area, and the optical fiber is located 0.05mm above the virus injection point (AP: -0.40mm; ML: + / - 2.95 mm; DV: 4.95 mm). Three weeks later, the next experiment was conducted. After the end of the experiment, the position of virus expression was confirmed, and the corresponding behavioral data was analyzed after observing whether the fluorescent expression of virus was in the target brain region.

Bilateral BLA cannula (O.D. 0.30 mm / 2.4 / M3.5 Arthur c., 62004, RWD life science co., LTD., shenzhen, China) was implanted the same as described above. The lateral ventricular cannula (O.D.0.41mm-27G/Pedestal 6mm/M3.5,62004, RWD Life Sciences Co., LTD., Shenzhen, China) was inserted as described previously with EEG electrodes embedded at the same time.

CTB-555 100nl (1μg/μl, BrainVTA Technology Co., LTD., Wuhan, China) was injected in DR (AP−4.55mm, ML−0.44mm, DV−2.80mm,10° right) or left BLA(AP: -0.40mm; ML: + / - 2.95 mm; DV: -5.00mm) with a total content of 100nL for retrograde labeling of projection neurons, and then perfused after 1 week.

2.4 Pharmacological and optogenetics experiments

2.4.1 Effect of intraperitoneal and BLA nuclear microinjection of 5-HTP on sevoflurane anesthesia induction time, emergency time and calcium signal of 5-HT neurons in BLA

5-HTP is the precursor of 5-hydroxytryptamine, which is soluble in normal saline. C57BL/6J mice were intraperitoneally injected with 5-HTP (50mg/kg, 100mg/kg), and injected again 24 hours later.One hour later, the mice were placed in the anesthesia box for induction and maintenance, and the induction time was recorded. Anesthesia was maintained for 30 minutes, and the emergency time was recorded then. The mouse in each group(vehicle, 50mg/kg, 100mg/kg) was subjected to three experiments, with complete metabolism of sevoflurane at an interval of one week.

One week after the implantation of bilateral cannulas in 8-week-old C57BL/6J mice, the BLA nuclear microinjection experiment was conducted. The mice were placed in the anesthesia box for anesthesia induction and the induction time was recorded. After 15 minutes of anesthesia, 200nl of 5-HTP (5mg/kg, 10mg/kg) was injected into the bilateral cannulas of BLA. Anesthesia was stopped at 30 minutes, and the emergency time was recorded. Each mouse in different group (vehicle, 5mg/kg, 10mg/kg) was subjected to three experiments, with complete metabolism of sevoflurane at an interval of one week.

2.4.2 Effect of photostimulation of 5-HT neurons in BLA on induction time and emergency time of sevoflurane anesthesia

The experiment was performed in 8-week-old C57BL/6J mice 3 weeks after virus injection and 1 week after fiber implantation. The mice were placed in the anesthesia box for 30min before anesthesia induction and the induction time of anesthesia was recorded. At the 15th or 20th minute of anesthesia maintenance, the

mice were exposed to blue light photostimulation (465 nm, 20 Hz, 20ms pulse, 10mW or 15mW) for 10 min or 15 min. After anesthesia maintenance for 30min, the anesthesia was stopped and the emergency time was recorded. The mouse in each group was subjected to three experiments, with complete metabolism of sevoflurane at an interval of one week.

2.4.3 Effects of lateral ventricle injection 5-HT1A receptor antagonist and photostimulation of BLA 5-HT neurons on the sevoflurane anesthesia induction time, emergency time and electroencephalogram (EEG)

The experiment was performed in 8-week-old C57BL/6J mice 3 weeks after virus injection and 1 week after lateral ventricle cannula implantation. EEG recording was started 5 minutes prior to induction. After injecting 5-HT1A receptor antagonist WAY 100635 (10mg/ml) through the lateral ventricle cannula, the mice were put into the anesthesia box and the induction time was recorded. At the 15th minute of anesthesia maintenance, the mice were exposed to blue light photostimulation (465nm, 15mW, 20Hz, 20ms pulse) for 15min. After 30 minutes of anesthesia, anesthesia was stopped and the emergency time was recorded. After the recovery of righting reflex, EEG was recorded for another 10 minutes. The mouse in each group (vehicle+no light group, 1A (-)+no light group, vehicle+light group, 1A (-)+light group) was subjected to four experiments, with complete metabolism of sevoflurane at an interval of one week.1A (-)= WAY 100635

2.5 Fiber photometry

2.5.1 Calcium signal changes of 5-HT neurons in BLA at different stages under sevoflurane anesthesia

The experiment was performed in 8-week-old C57BL/6J mice 3 weeks after virus injection and 1 week after optical fiber implantation. The mice were placed in the anesthesia box and recorded calcium signal 5min prior to induction when they were awake. Then the anesthesia induction was conducted and maintenance lasted for 30min. The induction time and emergency time was recorded at the same time. After the recovery of righting reflex, the experiment was stopped after 10min of optical fiber recording.

2.5.2 Calcium signal changes of 5-HT neurons in BLA under sevoflurane anesthesia after intraperitoneal injection of 5-HTP

The experiment was performed in 8-week-old C57BL/6J mice 3 weeks after virus injection and 1 week after optical fiber implantation. C57BL/6J mice were intraperitoneally injected with 5-HTP (50mg/kg, 100mg/kg), and injected again 24 hours later. One hour later, the mice were placed in the anesthesia box for induction and maintenance, and the induction time was recorded. The recording of calcium signal was started 5min prior to induction when they were awake. After 30 minutes of anesthesia, the anesthesia was stopped and the emergency time was recorded. After the recovery of righting reflex, the experiment was stopped after 10min of optical fiber recording. The mouse in each group was subjected to experiments twice (vehicle group, 10mg/kg group) with one week interval between each experiment to completely metabolize sevoflurane.

2.5.3 Changes of calcium signal and c-fos activation of 5-HT neurons in BLA under sevoflurane anesthesia after blue light activation of DRN

The experiment was performed in 8-week-old C57BL/6J mice 3 weeks after virus injection and 1 week after optical fiber implantation. The mice were placed in the anesthesia box and recorded for 5min prior to induction when they were awake. Then the anesthesia induction was conducted and the induction time was recorded at the same time. At 15min of maintenance, the mice received blue light photostimulation (465nm, 15mW, 20Hz, 20ms pulse) in DRN for 15 min. After 30min maintenance, the anesthesia was stopped and the emergency time was recorded. After the recovery of righting reflex, the optical fiber recording was continued for 10min.

2.6 Immunohistochemistry

The placement of the optical fiber cannula tip including intracerebroventricular (ICV) and microinjection of 5-HTP with bilateral BLA in each implanted mouse was verified by histology. After the experiment, C57BL/6J mice were sacrificed and perfused with PBS and 4% PFA. After saturated in 30% sucrose (24h), each brain was sectioned into 35μm thickness of coronal slices with a freezing microtome (CM30503,

Leica Biosystems, BuffaloGrove, IL, USA), the sections were first washed in PBS 5mins for 3 times and then incubated in blocking solution containing 10% normal donkey serum (017-000-121, Jackson ImmunoResearch, West Grove, PA), 1% bovine serum albumen (A2153, Sigma-Aldrich, St. Louis, MO), 0.3% Triton X-100 in PBS for 2 h at room temperature. Then, for c-fos or TPH2 staining in DR or BLA, sections were incubated at 4°C overnight in rabbit anti-c-fos(1:1000 dilution, 2250T Rabbit mAb , Cell Signaling Technolog, Danvers, Massachusetts, USA) primary antibody or mouse anti-TPH2 (1:100 dilution, T0678, Sigma-Aldrich, St. Louis, MO) primary antibody and donkey anti-mouse Alexa 546 (1:1000; A10036, Thermo Fisher Scientific, Waltham, MA, USA) secondary antibody or goat anti-rabbit cy5 (1:1000; A10523, Thermo Fisher Scientific, Waltham, MA, USA) secondary antibody for 2h at room temperature. After washing with PBS 15mins for 3 times, the sections were mounted onto glass slides and incubated in DAPI (1:4000;Cat# C1002; Beyotime Biotechnology; Shanghai, China) 7mins at room temperature.Finally, the glass slides were sealed sheet by Anti-fluorescence attenuating tablet.All images were taken with Nikon A1 laser-scanning confocal microscope (Nikon, Tokyo, Japan).The numbers of immunopositive cells were counted and analyzed using ImageJ (NIH, Baltimore, MD). It is worth noting that the mouse of the implantation placement out of the target of brain structure will be abandoned in our experiments. The positive cells co-expression c-fos,and TPH2 were counted as previously described.

2.7 Data statistics and analysis

The experimental data were reported as mean ± SD. Shapiro-wilk normality test was performed for all experimental data before data analysis. Comparison between the two groups: If the data conformed to the normal distribution, Student t-test was used, including independent sample T-test and paired sample T-test. If the data did not meet the normal distribution, Mann-Whitney U or Wilcoxon signed-rank test was used. Levene test was used to detect the homogeneity of square difference. After the data met the normal distribution and homogeneity of variance, one-way ANOVA analysis was used for the comparison of three or more groups, and two-way ANOVA analysis and Bonferroni's test were used for the comparison between two factors and

different groups. Statistical significance was inferred if $p < 0.05$. GraphPad Prism TM 8.0 and SPSS version 26.0 were used for statistical analysis of data in this study.

Results

3.1 Sevoflurane anesthesia modeling of C57BL/6J mice

The time to LORR of mice exposed to different sevoflurane concentrations was different (Fig 1B). In order to determine the appropriate concentration of sevoflurane, we normalized the Induce time of mice in each group, and took the drug concentration corresponding to the median Induce time of all mice, i.e. 2.55% sevoflurane, as the induction and maintenance dosage for subsequent mice (Fig 1).

3.2 5-HT neuronal activity in BLA during maintenance period was significantly reduced based on photometry recordings

During sevoflurane anesthesia, calcium signals of 5-HT neurons in bilateral BLA infected with GCaMP6s were recorded by photometry (Fig 2). There was significant difference in peak $\Delta F/F$ of 5-HT neurons in BLA between the maintenance period and other stages ($p<0.05$, Fig2). These data indicates that the activity of 5-HT neuron in BLA may involve in the process of sevoflurane anesthesia.

3.3 5-HT neuronal activity in BLA during anesthesia was significantly increased by elevating the level of 5-HT

Compared with the vehicle group, intraperitoneal injection of 5-HTP with different concentrations had no significant difference in Induction time ($p>0.05$, Fig 3). The group treated with 5-HTP 100mg/kg had longer Induce time than 50mg/kg ($p<0.05$, Fig 3). Compared with the vehicle group, the emergency time was significantly reduced after IP 100mg/kg 5-HTP ($p<0.001$). And compared with the group IP 100mg/kg 5-HTP, the emergency time was significantly increased after IP delivery of 5-HTP at a dosage of 50mg/kg ($p<0.01$, Fig 3).

To further explore the role of 5-HT neurons in BLA, we microinjected 400nL vehicle and 5-HTP in BLA. Compared with the vehicle group, microinjection 5-HTP in BLA had no significant difference in Induction time ($p>0.05$, Fig 4 E). However, compared with the vehicle group, the emergency time was significantly reduced after microinjection 10mg/ml 5-HTP ($p<0.001$). And compared with the group

microinjection 10mg/ml 5-HTP, the emergency time was significantly increased after microinjection 5-HTP at a dosage of 5mg/ml ($p<0.01$, Fig 4).

There was significant difference in peak ΔF/F of 5-HT neurons in BLA between the vehicle group and the group IP 100mg/kg 5-HTP during RORR ($p<0.01$, Fig 3G-H). These data indicates that 5-HT neuron in BLA may have an important impact on the process of sevoflurane anesthesia, especially the recovery stage.

3.4 Effect of activation 5-HT neurons in BLA on Induction time and Emergency time of sevoflurane anesthesia

We examined the effect of selective enhancement of 5-HT neurotransmission on Induce time and Emergency time by applying photostimulation (blue light: 10min, 15mW; 15min, 15mW; 15min, 10mW) to 5-HT neurons in BLA. Compared with the vehicle group, photostimulation of the BLA (10min, 15mW; 15min, 15mW; 15min, 10mW) had no significant difference in Induction time ($p>0.05$, Fig 5 B). The group treated with 5-HTP 100mg/kg had the longer Induce time than 50mg/kg ($p>0.05$, Fig 5 C and 5 F). Compared with the vehicle group, the Emergency time was significantly reduced after photostimulation of the BLA (blue light, 15min, 15mW) ($p<0.001$). And compared with the group photostimulation of the BLA (blue light, 15min, 15mW), the Emergency time was significantly increased after photostimulation of the BLA (blue light: 10min, 15mW; 15min, 10mW) ($p<0.05$, Fig 4D; $p<0.01$, Fig 5 G). There was no significance in Induce time in the following group respectively: no PS, left PS, right PS and bilateral PS ($p>0.05$, Fig 5 E). And compared with the no PS group, the Emergency time was significantly decreased in the group with left PS, right PS or bilateral PS ($p<0.001$, Fig 5 H), indicating activation of 5-HT neuron located in BLA could promote the recovery of anesthesia in C57BL/6J mice.

3.5 EEG activity upon optogenetic activation of 5-HT neurons in BLA-mediated reduction of the Emergency time during sevoflurane anesthesia

pAAV-TPH2 PRO-ChETA-EYFP-WPRES-PAS was delivered into BLA 3 weeks before anesthesia, and an optical fiber with a headstage for EEG was implanted 1 week before experiments. The mice were divided into three groups: no PS, PS (10mW, 15min), PS (15mW, 15min). The activity of cortical EEG of three groups decreased

significantly after LORR, and kept at a low level during the maintenance of anesthesia. During the recovery stage, the cortical EEG recovered, but was still lower than that before anesthesia (Fig 6 A).

For Delta wave, the average proportion in the three groups during anesthesia had no significant difference ($p>0.05$, Fig 6 B). As for Alpha wave, the average proportion of Alpha wave in maintenance phase was significantly higher than that in the recovery phase in the vehicle group ($P<0.001$), PS (10mW, 15min) ($P<0.05$) and PS (15mW, 15min) ($P<0.01$). And the average proportion of Alpha wave in PS (15mW, 15min) during wakening phase was significantly higher than that in the recovery phase ($P<0.01$, Fig 6 C). For Beta wave, the group treated with PS (15mW, 15min) in the awake state was significantly lower than that in the anesthesia or recovery state ($P<0.05$, $P<0.05$, Figure 5 D). For Theta wave, the percentage of Theta wave in vehicle group during maintenance phase was significantly higher than wakefulness phase ($P<0.05$) and recovery phase ($P<0.05$). And the percentage of Theta wave in PS (10mW, 15min) and PS (15mW, 15min) during maintenance phase was significantly higher than recovery phase ($P<0.05$, $P<0.05$, Fig 6 E).

As for Gamma wave, there was no statistical difference in PS (10mW, 15min) during anesthesia. In the vehicle group, the Gamma wave proportion was significantly lower in the maintenance stage than that in wakefulness ($P<0.05$) and recovery ($P<0.001$). In the group with PS (10mW, 15min), the Gamma wave proportion was significantly higher in the wakefulness than that in maintenance ($P<0.01$) and recovery ($P<0.05$). In the group with PS (15mW, 15min), the Gamma wave proportion was significantly higher in the recovery than that in maintenance ($P<0.001$, Fig 6 F). These indicates EEG activity alters in different stages and different wave change in different ways and degrees.

3.6 EEG activity upon optogenetic activation of 5-HT neurons in BLA-mediated reduction of the Emergency time during sevoflurane anesthesia

pAAV-TPH2 PRO-ChETA-EYFP-WPRES-PAS was delivered into BLA 3 weeks before anesthesia, and an optical fiber with a headstage for EEG was implanted 1 week before experiments. The mice were divided into three groups: no PS, PS (15mW,

10min), PS (15mW, 15min). The activity of cortical EEG of three groups decreased significantly after LORR, and kept at a low level during the maintenance of anesthesia (Fig 7 A).

For Delta and Theta wave, the average proportion in the three groups during anesthesia had no significant difference ($p>0.05$, Fig 6 B and 6 E). As for Alpha wave, the average proportion of Alpha wave in vehicle group during maintenance phase was significantly higher than that in the recovery phase ($P<0.05$). And the average proportion of Alpha wave in PS (15mW, 10min) and PS (15mW, 15min) during maintenance phase was significantly higher than that in the recovery phase ($P<0.05$, $P<0.05$, Fig 7 C). For Beta wave, the vehicle group in the awake state was significantly lower than that in the anesthesia state ($P<0.05$, Figure 7 D). As for Gamma wave, the Gamma wave proportion in vehicle group was significantly higher in the awake stage than that in maintenance ($P<0.05$) and recovery ($P<0.05$). In the group with PS (15mW, 10min), the Gamma wave proportion was significantly higher in the recovery than that in maintenance ($P<0.05$). In the group with PS (15mW, 15min), the Gamma wave proportion was significantly lower in the maintenance than that in wakefulness ($P<0.05$) and recovery stage ($P<0.01$, Fig 7 F). These indicates EEG activity alters in different stages, especially Gamma wave.

3.7 Effect of ICV 5-HT 1A receptor antagonist on Induction time and Emergency time of sevoflurane anesthesia

pAAV-TPH2 PRO-ChETA-EYFP-WPRES-PAS was delivered into BLA 3 weeks before anesthesia, and a lateral ventricle cannula as well as an optical fiber were implanted. The mice were divided into four groups: vehicle + no PS, 1A(-) + no PS, vehicle + PS, 1A(-) + PS. The results showed the administration of 5-HT 1A receptor antagonist and photostimulation 5-HT neuron in BLA had no significant effect on the induction time of sevoflurane ($P>0.05$, Fig 8 B).

As for the Emergency time, the group treated with 1A(-) + no PS was significantly longer than these treated with vehicle + no PS ($P<0.05$) and vehicle + PS ($P<0.001$), indicating 5-HT1AR was involved in mediating the recovery of sevoflurane anesthesia. And the group treated with 1A(-) + PS had significant longer

Emergency time than the group received vehicle + PS, which suggested the suppressive effect of 5-HT 1AR could reverse the positive effect of activation 5-HT neurons in BLA.

3.8 The effect of ICV 5-HT 1A receptor antagonist on EEG activity

rAAV-TPH2-GCaMP6S-WPRE-hGH was delivered into BLA 3 weeks before anesthesia, an optical fiber, and an ICV cannula microinjecting 5-HT 1A(-) with a headstage for EEG was implanted 1 week before experiments. The mice were divided into four groups: vehicle + no PS, vehicle + PS, 1A(-) + no PS and 1A(-) + PS. The activity of cortical EEG in each group decreased significantly after LORR, and kept at a low level during the maintenance of anesthesia (Fig 9 A).

For Beta and Theta wave, the average proportion in the four groups during anesthesia had no significant difference ($p>0.05$, Fig 9 D and 9 E). As for Delta wave, the average proportion of Delta wave in 1A(-) + no PS group during maintenance phase was significantly lower than that in the awakening phase ($P<0.05$) and recovery phase ($P<0.05$, Figure 9 B), suggesting 5-HT 1A receptor may involve in mediating EEG activity during sevoflurane anesthesia. And the average proportion of Alpha wave in 1A(-) + no PS group during maintenance phase was significantly lower than that in the wakefulness phase ($P<0.05$, Fig9 C).

As for Gamma wave, the Gamma wave proportion in 1A(-) + no PS group was statistically lower in the anesthesia stage than that in awake ($P<0.001$) and recovery state ($P<0.001$) and the EEG activity did not return to the same level after RORR ($P<0.001$). In the group with 1A(-) + PS, the Gamma wave proportion was significantly higher in the recovery than that in maintenance ($P<0.01$, Fig 9 F). These indicates 5-HT 1A receptor in BLA may participate in mediating EEG activity during sevoflurane anesthesia, especially Gamma wave.

3.9 5-HT neuron projection from DR to BLA was established by the application of the nerve tracer CTB-555.

To further retrograde the 5-HT neuron projection in BLA, we microinjected CTB-555 in BLA and then perfused after 1 week. Immunohistochemical results suggested that DR 5-HT neuron might project to BLA (FIG 10).

3.10 5-HT neural projection from DR to BLA involved in reducing the Emergency time of sevoflurane anesthesia

pAAV-TPH2 PRO-ChETA-EYFP-WPRES-PAS was delivered into DR 3 weeks before anesthesia, and optical fibers were implanted 1 week before experiments (Figure 11A). We selectively activated 5-HT neuron in DR by applying photostimulation.

Induction time in control group without PS and group with PS showed no statistical difference. Compared with the control group without PS, there was significant difference in the Emergency time of mice in experimental group with PS ($P<0.001$). Quantification of c-fos(+)/TPH2(+) cells in BLA with PS in DR were significantly more than these cells in BLA without PS in DR ($p<0.05$, Figure 11B).

Calcium signaling within neurons of bilateral BLA was recorded by photometry in mice infected with GCaMP6s in the group treated with or without photostimulation in DR during maintenance stage (Figure 11 E). We observed obvious difference in peak $\Delta F/F$ in BLA between the control group and photostimulation group (Fig 10F). Compared with the vehicle group, peak $\Delta F/F$ of RORR was significantly increased in the photostimulation group ($p<0.05$, Fig 11 G). These data indicate that 5-HT neural projection from DR to BLA involved in reducing the Emergency time of sevoflurane anesthesia.

Discussion

The researches on the specific mechanism of arousal from general anesthesia, and the mechanism of reversible loss of consciousness during general anesthesia is the focus of the field of anesthesia. In this study, we used optogenetic techniques and intraperitoneal injection and intracerebroventricular injection to reveal the role of BLA in emergence from general anesthesia. And the effects of anesthesia and excited the serotonin neurons in BLA on the electroencephalogram (EEG) of the mice were observed by cortical EEG recording. The present results demonstrated that the stimulation of BLA could reduce the emergency time from general anesthesia, which might through 5-HT neurons, particularly in the DR.

General anesthetics have been used for more than 170 years, which can cause

loss of consciousness and analgesia, and ensure the success of surgery. However, the mechanism of general anesthesia is still unclear. The journal Science listed "How general anesthetics work" as one of 125 frontier questions in science. Using D1R-Cre mice, the study found that dopamine D1R-positive neurons showed decreased activity during sevoflurane anesthesia induction and increased activity during emergence by in vivo fiber calcium signals and EEG-EMG recordings. Blue light specifically activates D1R positive neurons in the nucleus accumbens of mice under continuous stable anesthesia, which can rapidly induce cerebral cortex activation and behavioral awakening[27].

It suggests that the mechanism of general anesthetics may intersect with the sleep-wake regulatory neural circuit. The neural networks, involved in the mechanism of general anesthetic agents and sleep-wake, are comprised of the basal forebrain, the preoptic area of the hypothalamus which contains the ventrolateral preoptic (VLPO) nucleus, the posterolateral region of the hypothalamus, the brainstem, and the thalamus[28]. The lateral hypothalamic area (LHA) contains wake-promoting orexinergic (hypocretin) neurons, which is essential for stabilizing the sleep-wake state, activing during wakeful and REM sleep, and capable of sending projections throughout the brain, including to the VLPO, to maintain wakeful state [29, 30, 31]. The prefrontal cortex (PFC) receives input fibers from the dorsomedial thalamus and has extensive connections with subcortical wakeing-related nuclei, including the serotonergic dorsal raphe nucleus (DR), the noradrenergic locus ceruleus (LC), the cholinergic basal forebrain, and the dopaminergic ventral dorsal tegmental area (VTA). Studies have shown that the inactivation of the PFC can delay the emergence from general anesthesia in rats, and the PFC also plays an important role in awakening. However, it should be noted that the role of the posterior cortex in awakening has also been confirmed in many other experiments[32].

BLA is associated with many behaviors, such as fear, aggression, learning, and memory [33]. From the amygdala (via the central nucleus) there is a massive projection to the brainstem regions involved in the arousal and REM waves and ponto-geniculo-occipital (PGO) waves [34, 35]. The BLA receives cortical and

subcortical inputs and projects to brainstem, hypothalamus, forebrain, and cortical regions associated with hormonal, autonomic, and behavioral aspects of stress responses and is also involved in the sleep-wake cycle [36, 37]. There are still few studies on the role of BLA in sleep-wake and general anesthesia mechanism, so we chose BLA as the target to explore the mechanism of emergence from general anesthesia.

5-HT neurons are widely distributed and projected in the central nervous system, and their physiological functions are complex due to their numerous receptor subtypes. In the study of sleep-wake regulation drugs, it is found that most drugs act through different subtypes of 5-HT receptor. Studies have shown that 5-HT in the hippocampus has a sleep-promoting effect by changing the content of 5-HT in the thalamic reticular nucleus and activating or inhibiting 5-HT1A receptors to produce sleep-promoting or wake-promoting effects. Microinjection of 5-HT1A receptor agonist into the DRN stimulated the autoreceptor of 5-HT1A, and increased REMS were found in cats and rats [38]. Injection of p-MMPI, a 5-HT1A receptor antagonist, into the DRN resulted in a reduction in REMS and spontaneous firing of DRN neurons. The 5-HT1B receptor in the medial preoptic nucleus also has a role in arousal. Studies have found that injection of 5-HT3 receptor agonist in DRN can reduce REMS and SWS and promote arousal[39]. However, injection of 5-HT6 receptor antagonist had no significant effect on REMS. After treatment with 5-HT7 receptor antagonist or knockdown of 5-HT7 gene, REM sleep time was reduced in rats, which was later found to be indirectly mediated by 5-HT1A receptor. Our previous study showed that activation of 5-HT 1A receptor by lateral ventricle and DR intranuclear injection can significantly shorten the emergence time of sevoflurane anesthesia. Earlier studies have suggested that 5-HT is a ‘sleep’ neurotransmitter as the lesion of the raphe nuclei leads to insomnia in cats[40]. The previous studies have shown that the extracellular level of 5-HT in BLA is lower during sleep than in waking which might be mediated by the serotonergic projection of the DRN to the BLA [41, 42]. Therefore, we investigated the relationship between BLA and 5-HT in DR during emergence from general anesthesia, and whether 5-HT 1A receptors play a major role in reducing the emergence time.

In addition to the role of 5-HT system in BLA regulation of emergence time of general anesthesia, norepinephrine (NE), synthesized by the neurons of brainstem locus ceruleus (LC) nuclei, may also be involved during the arousal in BLA. NE-containing LC neurons are interconnected with forebrain structures, including the amygdala, and has been implicated in the regulation of the sleep-wake cycle[43, 44, 45]. It has been shown that extracellular levels of NE in the LC and amygdala gradually decrease from wakefulness to slow wave sleep to REM sleep [46]. Therefore, the BLA may receive information from different neurotransmitters and brain regions, except 5-HT in DR, for integration at the same time. Further studies on the connections and projections between the BLA and other brain regions during the emergency of general anesthesia will be conducted in the future.

Figure Legends

Figure 1

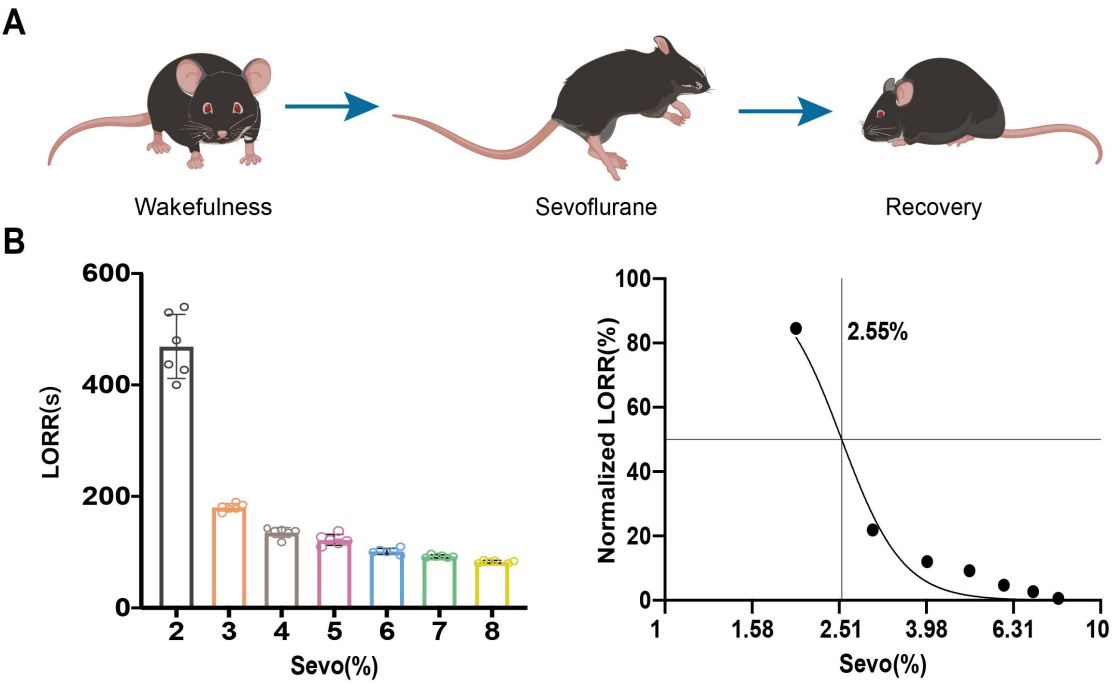

Figure1 Sevoflurane anesthesia modeling of C57BL/6J mice

A. The anesthesia process of C57BL/6J mice **B.** The time to LORR under different inhalation concentrations of sevoflurane (n=6 for each group). **C.** Normalization the Induce time of mice in each group. **LORR, loss of righting reflex; Sevo, sevoflurane**

Figure 2

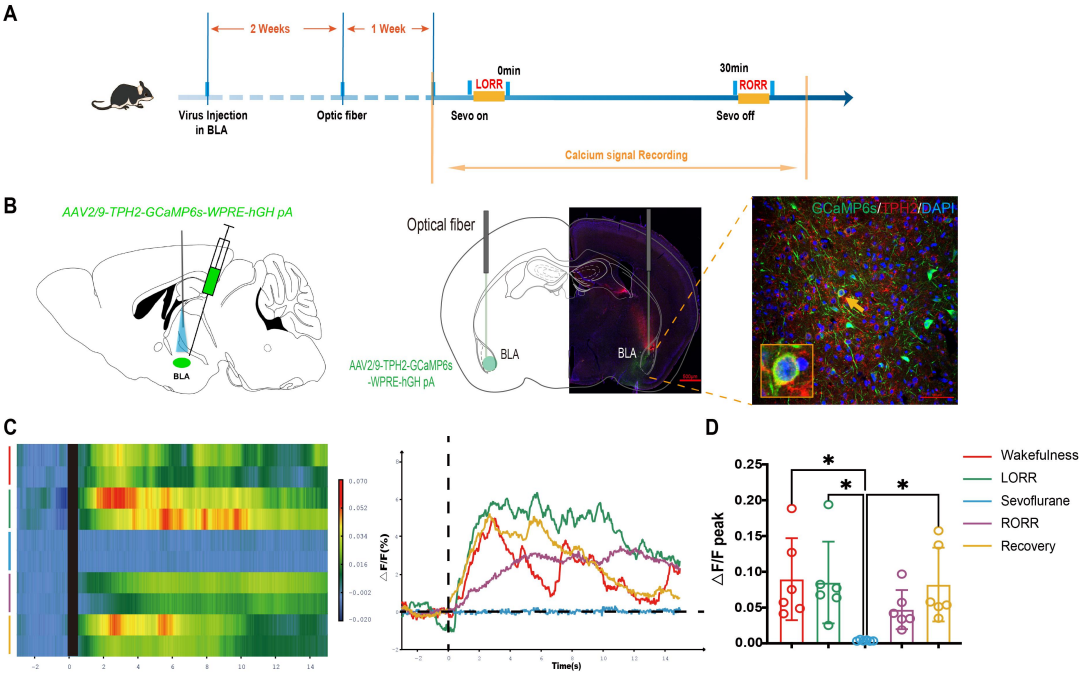

Figure2 Changes of calcium signaling in BLA 5-HT neurons during anesthesia

A. Schematic illustration of Photometric recordings **B.** A representative photomicrograph shows microinjection and optical fiber locations and the co-expression GCaMP6s and TPH2. **C.** The heatmap and statistical diagram of calcium signaling changes in bilateral BLA 5-HT neurons during sevoflurane anesthesia. **D.** Peak ΔF/F in BLA during the maintenance of anesthesia was significantly lower than that during the waking, induction and recovery periods. ***p<0.05**

Figure 3

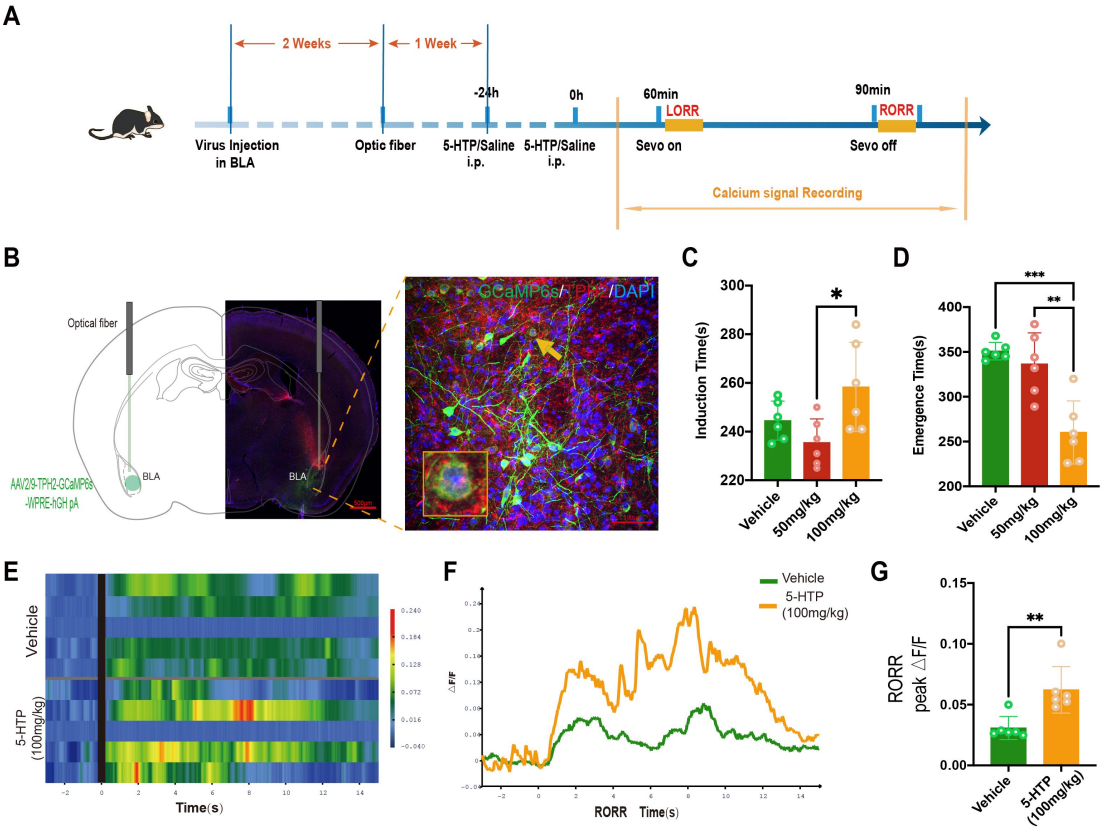

Figure 3 Effects of administration 5-HTP to elevate the level of 5-HT on the Changes of calcium signaling in BLA 5-HT neurons during anesthesia

A. Schematic illustration of Photometric recordings **B.** A representative photomicrograph shows microinjection and optical fiber locations and the co-expression GCaMP6s and TPH2. **C-D.** Compared with the vehicle group, intraperitoneal injection of 5-HTP with different concentrations had no significant difference in Induction time ($p>0.05$). The group treated with 5-HTP 100mg/kg had the longer Induce time than 50mg/kg ($p<0.05$). **E-F.** The heatmap and statistical diagram of calcium signaling changes in bilateral BLA 5-HT neurons during sevoflurane anesthesia with the treatment of 5-HTP and without the treatment of 5-HTP. **D.** Peak ΔF/F in BLA during the maintenance of anesthesia without the treatment of 5-HTP was significantly lower than that during the waking in the group with 5-HTP, induction and recovery periods. ***p<0.05**

Figure 4

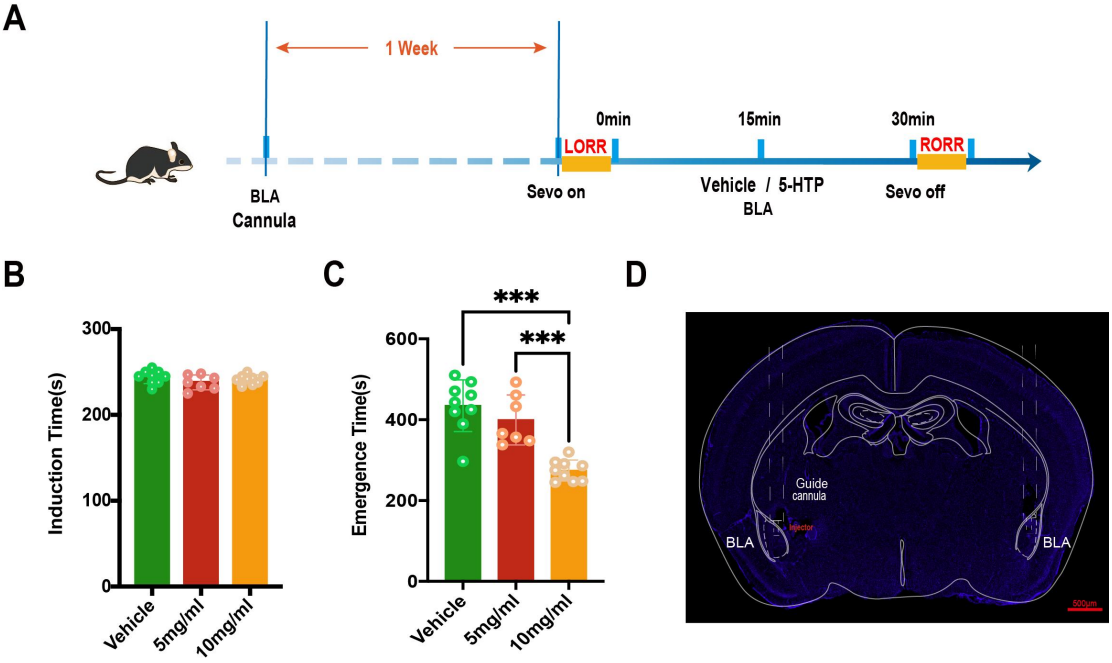

Figure 4 The difference of Induce time and Emergency time when elevating the level of 5-HT via IP and BLA microinjection 5-HTP

A. Schematic illustration of microinjection 5-HTP in BLA **B-C.** Effect of IP different concentrations of 5-HTP on Induction time and Emergency time **D.** A representative photomicrograph shows microinjection locations. **E-F.** Effect of microinjection different concentrations of 5-HTP in BLA on Induction time and Emergency time **G.** Peak ΔF/F of 5-HT neurons in BLA during RORR was significantly increased in the group treated with IP 100mg/kg 5-HTP. *****p<0.001, **p<0.01, *p<0.05, IP intraperitoneal injection, RORR recovery of righting reflex**

Figure 5

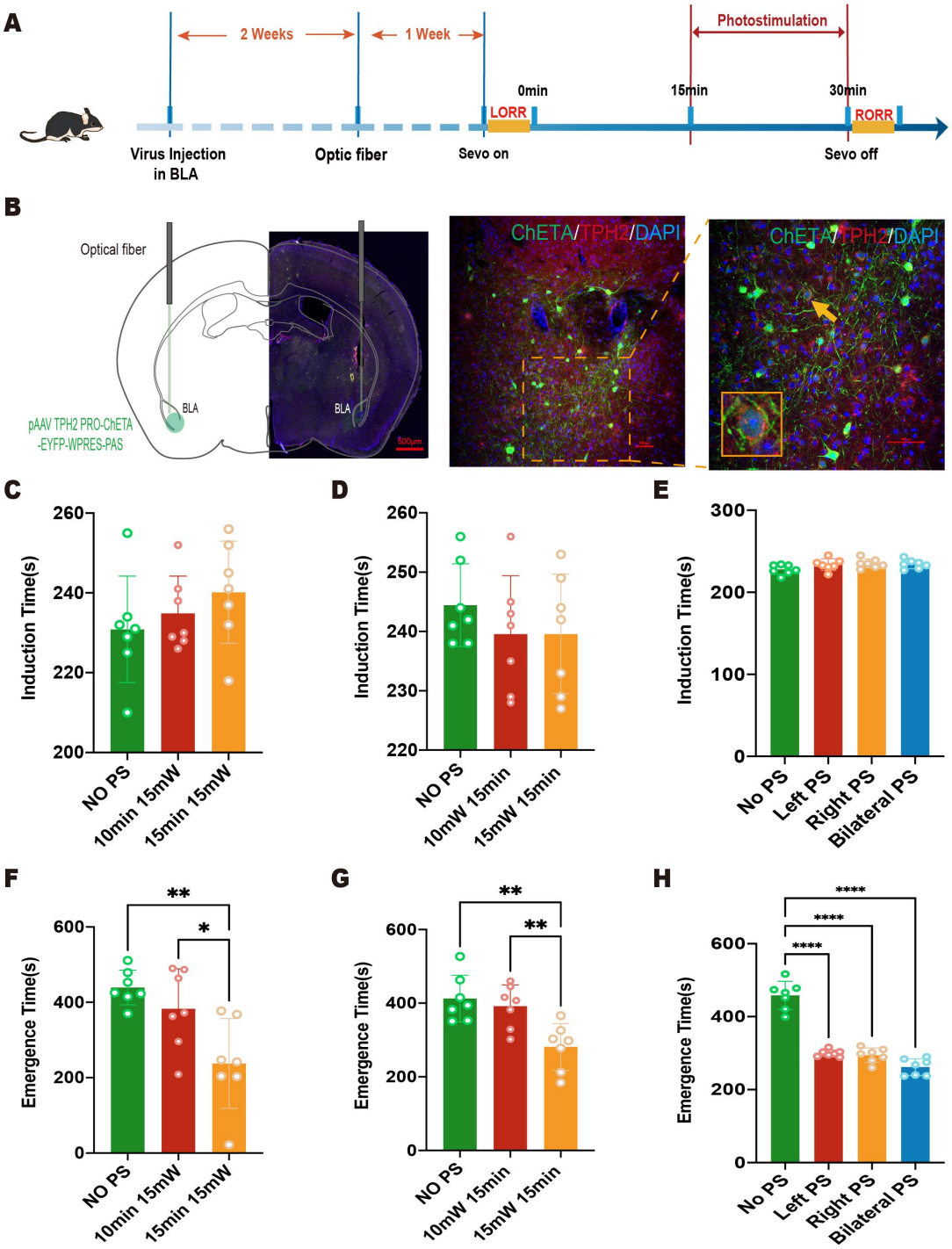

Figure 5 The difference of Induce time and Emergency time when photostimulating 5-HT neuron in BLA with different light parameters

A. Schematic illustration of photostimulation 5-HT neuron with different light parameters in BLA **B.** A representative photomicrograph shows the locations of optical fiber and virus expression. **C-D, F-G.** Effect of photostimulating 5-HT neuron in BLA (10min, 15mW; 15min, 15mW; 15min, 10mW) on Induction time and

Emergency time **E, H.** Effect of photostimulating 5-HT neuron in BLA (no PS, left PS, right PS, bilateral PS) on Induction time and Emergency time. ***p<0.001, **p<0.01, *p<0.05, PS photostimulation

Figure 6

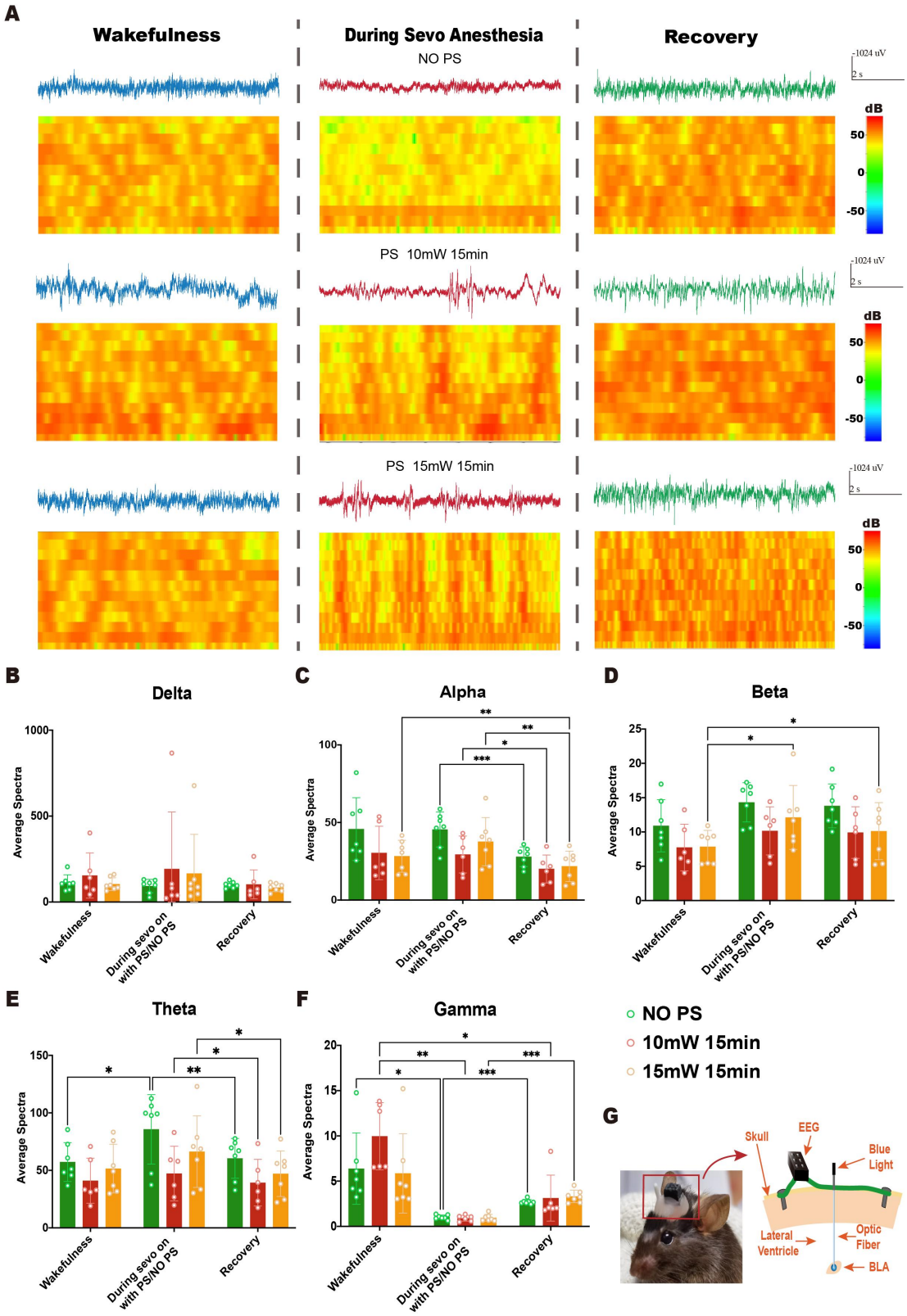

Figure 6 Effect of photogenetic activation of 5-HT neurons in BLA on EEG activity

A. EEG and spectrum of mice in vehicle group, PS (10mW, 15min) and PS (15mW, 15min) under awake, anesthetized and recovery states. **B-F.** Delta, Alpha, Beta, Theta and Gamma wave proportion of EEG in three groups of mice in different states **G.** Schematic Diagram of Mouse Cortical EEG Recording and optical fiber .***** p<0.001, ** p<0.01, * p<0.05, PS photostimulation**

Figure 7

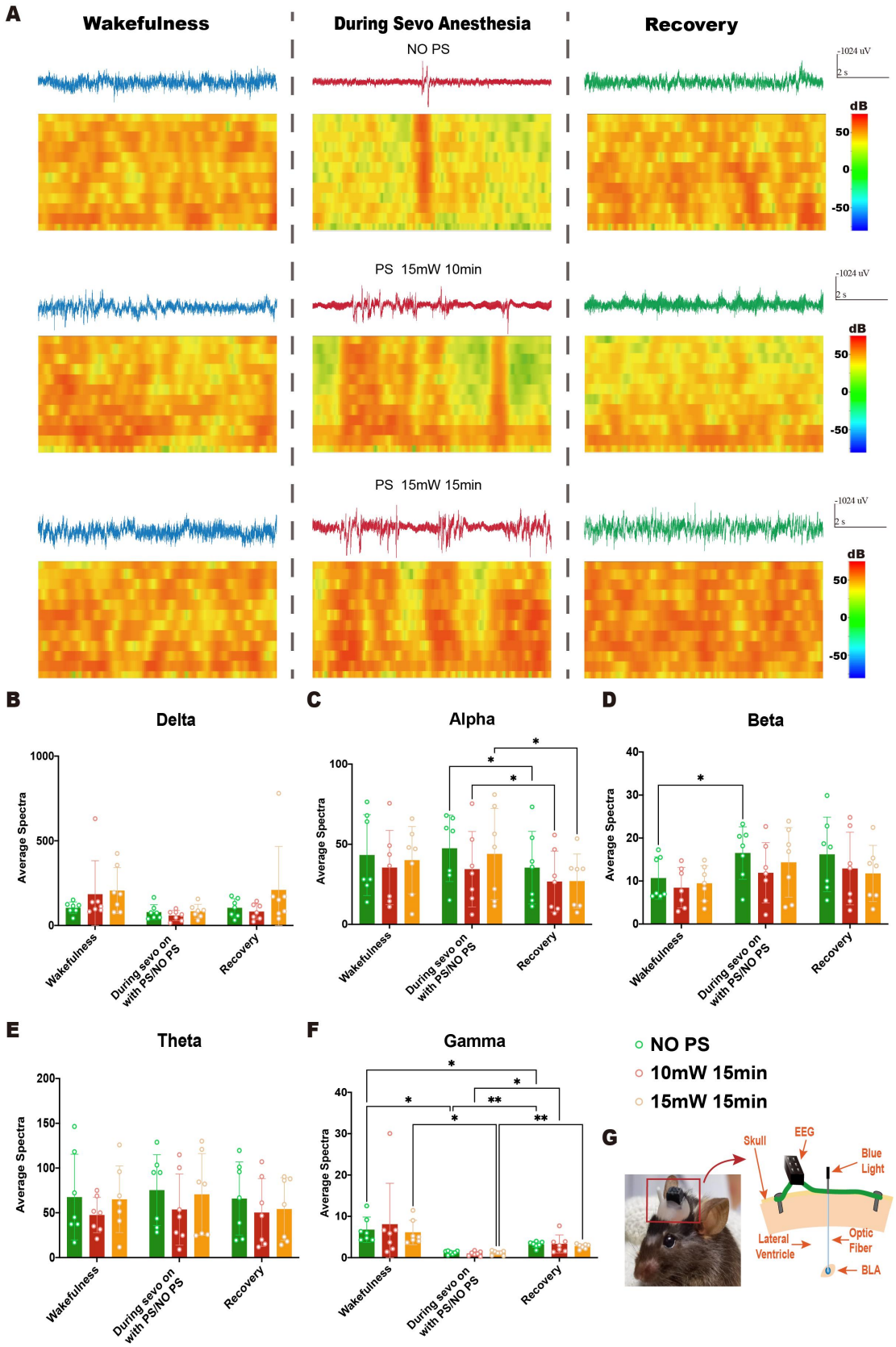

Figure 7 Effect of photogenetic activation of 5-HT neurons in BLA on EEG activity

A. EEG and spectrum of mice in vehicle group, PS (15mW, 10min) and PS (15mW, 15min) under awake, anesthetized and recovery states. **B-F.** Delta, Alpha, Beta, Theta and Gamma wave proportion of EEG in three groups of mice in different states **G.** Schematic Diagram of Mouse Cortical EEG Recording and optical fiber ***p<0.001, **p<0.01, *p<0.05, PS photostimulation

Figure 8

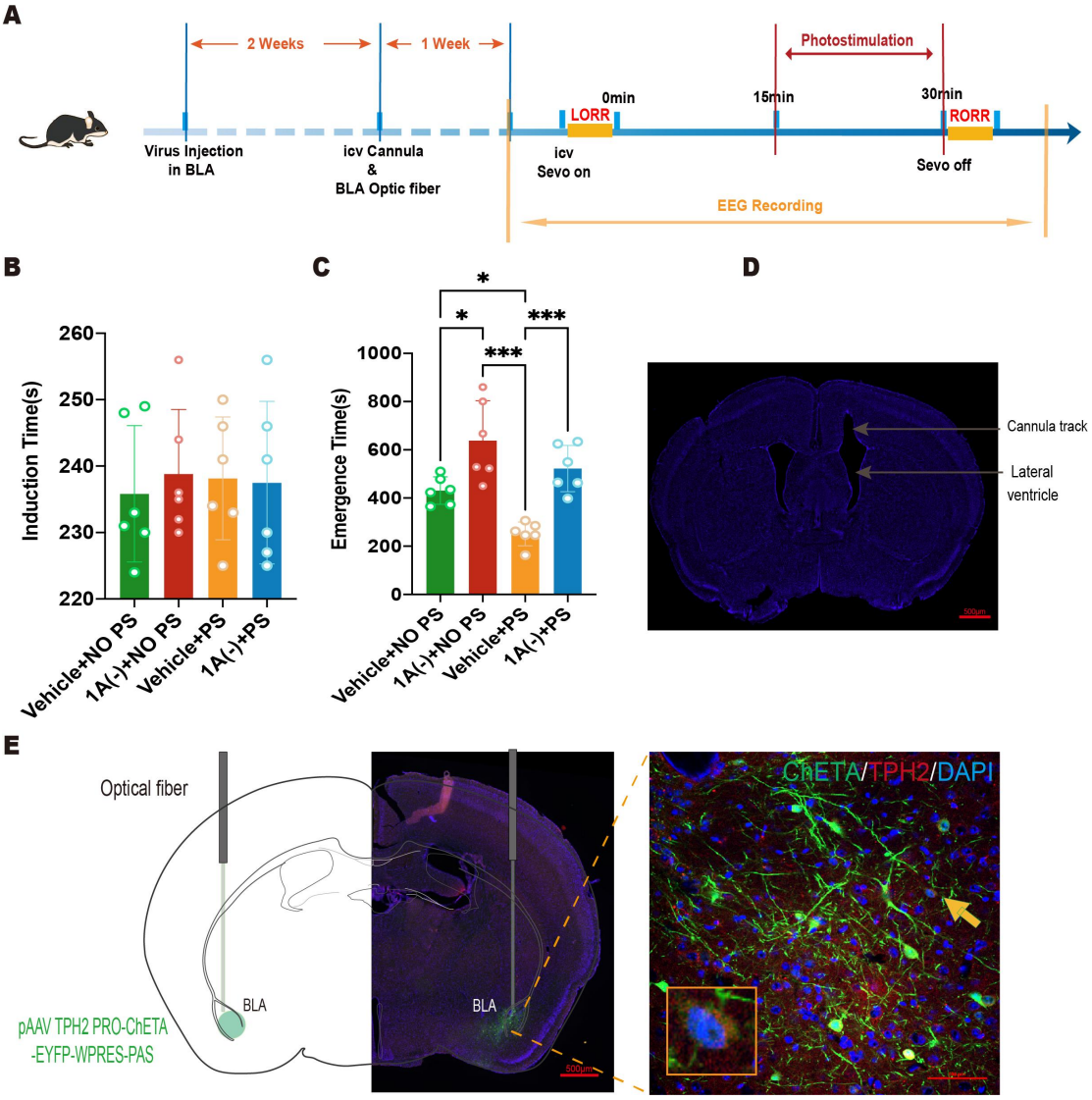

Figure 8 The suppressive effect of ICV 5-HT 1AR on Induce time and Emergency time

A. Experimental protocol for lateral ventricle administration and optogenetic stimulation of BLA 5-HT neurons. **B-C.** The effect of 5-HT 1AR and BLA 5-HT neuron photostimulation on Induce time and Emergency time of sevoflurane anesthesia **D.** A representative photomicrograph shows the locations of ICV cannula

and optic fiber. **E.** A representative photomicrograph shows the locations of optical fiber and virus expression. 1A (-)= WAY 100635; *****p<0.001, **p<0.01, *p<0.05, PS=photostimulation, ICV= intracerebroventricular**

Figure 9

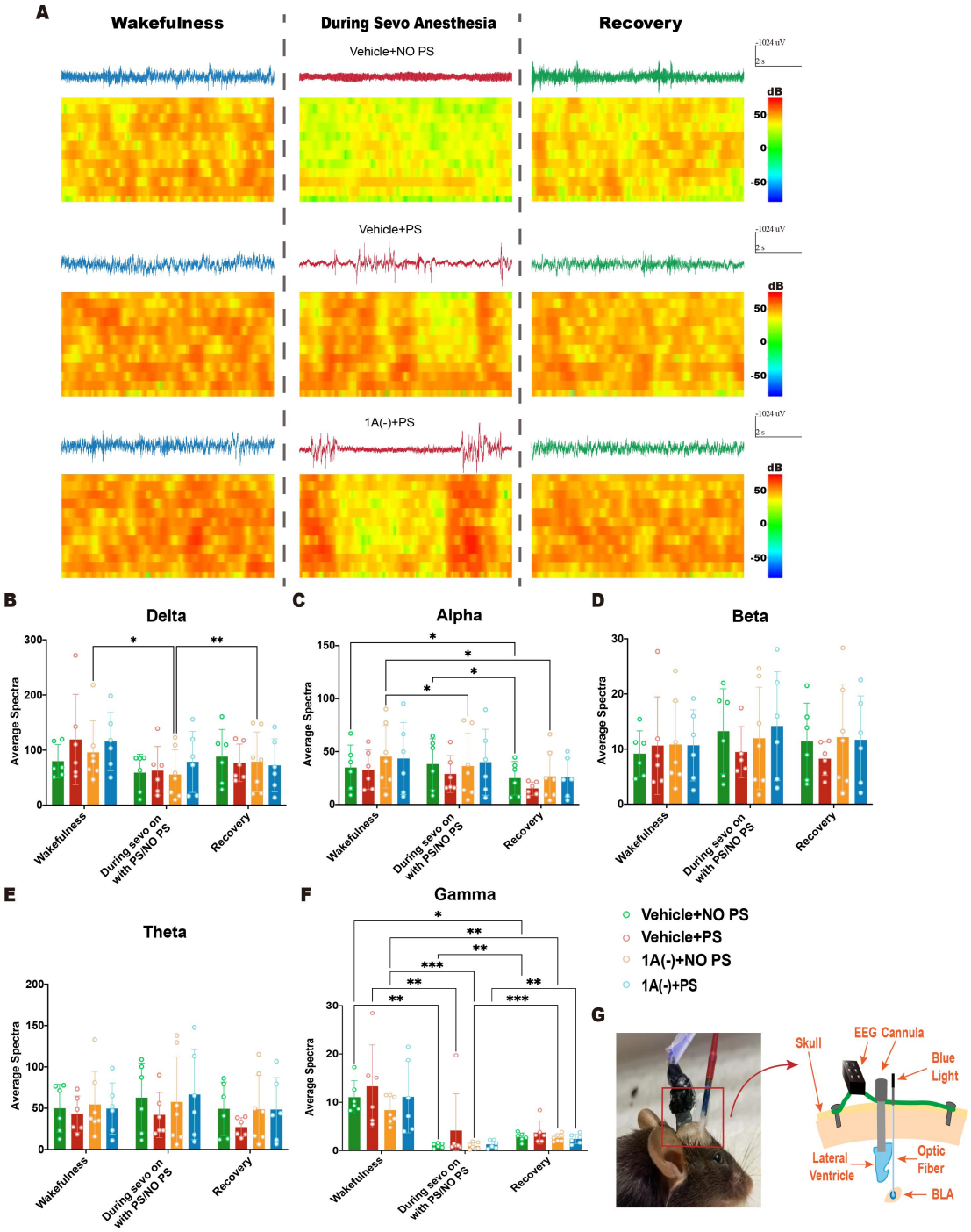

Figure 9 Effect of ICV 5-HT 1AR and photogenetic activation of 5-HT neurons in BLA on EEG activity

A. EEG and spectrum of mice in vehicle group + no PS, vehicle + PS, 1A(-) + no PS

and 1A(-) + PS under awake, anesthetized and recovery states. **B-F.** Delta, Alpha, Beta, Theta and Gamma wave proportion of EEG in four groups of mice in different states **G.** Schematic Diagram of Mouse Cortical EEG Recording, ICV cannula and optical fiber. 1A (-)= WAY 100635; *****p<0.001, **p<0.01, *p<0.05, PS=photostimulation, ICV= intracerebroventricular**

Figure 10

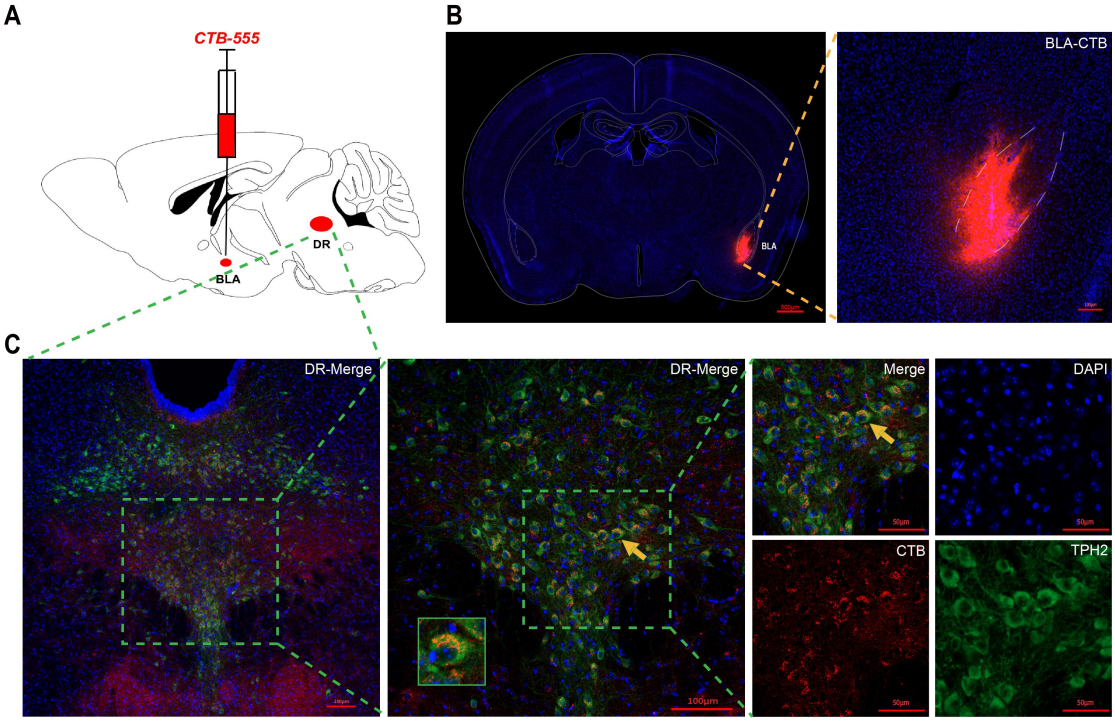

Figure 10 Neural projection from DR to BLA was established by microinjecting nerve tracer CTB-555 in BLA

A-B. Representative coronal brain slice, showing the location of CTB-555 injected in BLA. **C.** Projection from DR to BLA with co-expression of CTB-555, TPH2 and DAPI.

Figure 11

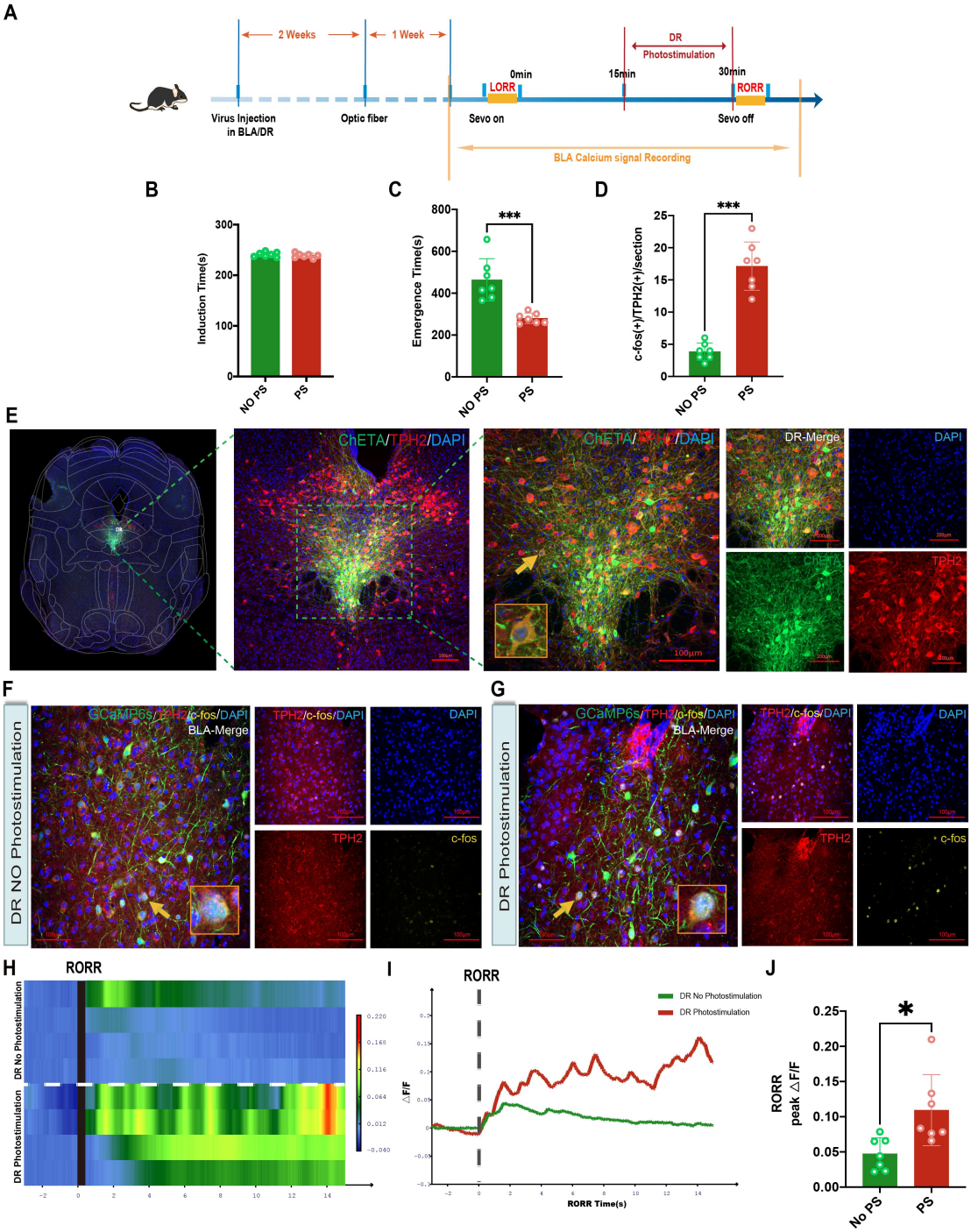

Figure 11 Photostimulation of DR 5-HT neuron influenced the expression of c-fos in BLA and calcium signaling in BLA 5-HT neuron during RORR

A. Experimental protocol for BLA 5-HT neuron photometric recordings and optogenetic stimulation of DR 5-HT neurons. **B.** The effect of activating DR 5-HT neuron on the Induce time, Emergency time during sevoflurane anesthesia and the expression of c-fos in BLA **C.** Shown are representative images of the tracks of optic

fibers implanted into DR and staining for ChETA, TPH2 and DAPI in the DR. **D.** Representative images staining for c-fos, TPH2 and DAPI in DR **E.** The photometry recordings of the group with DR PS and without DR PS during the period of RORR **F-G.** There was significant difference in peak ΔF/F of BLA between DR with PS and DR with PS. ***p<0.05, PS= photostimulation**

Table 1

summary of experimental groups of C57BL/6J mice

Figure	Experimental groups	Number of mice
Fig1	2% Sevo	6
	3% Sevo	6
	4% Sevo	6
	5% Sevo	6
	6% Sevo	6
	7% Sevo	6
	8% Sevo	6
Fig2	2.5%Sevo	6
Fig3	Vehicle	6
	5-HTP(50mg/kg)	6
	5-HTP(100mg/kg)	6
Fig4	vehicle	7
	5-HTP(5mg/kg)	7
	5-HTP(10mg/kg)	7
Fig5	NO Photostimulation	7
	10mw15min with Photostimulation	7
	15mw 15min with Photostimulation	7
	NO Photostimulation	7
	10min 15mw with Photostimulation	7
	15min 15mw with Photostimulation	7
	NO Photostimulation	7
	Left 15mw 15min with Photostimulation	7
	Right 15mw 15min with Photostimulation	7
	Bilateral 15mw 15min with Photostimulation	7
Fig6	NO Photostimulation	7
	10mw15min with Photostimulation	7
	15mw 15min with Photostimulation	7
Fig7	NO Photostimulation	7
	10min 15mw with Photostimulation	7
	15min 15mw with Photostimulation	7
Fig 8/9	Vehicle+NO PS	6
	1A(-)+NO PS	6
	Vehicle+PS	6
	1A(-)+PS	6
Fig 10	BLA CTB	3
Fig 11	NO Photostimulation	7
	Photostilulation	7
	quantification of c-fos(+)/TPH2(+) cells	7

Table 2
statistical analysis

Figure	Comparisons	Test
Fig1	Sevo(%)-Normalized LORR(%)	Nonlinear Regression
Fig2	△F/F peak	Ordinary one-way ANOVA
Fig3	Induce time	Ordinary one-way ANOVA
	Emergence time	Ordinary one-way ANOVA
	RORR △F/F peak	Unpaired t test
Fig4	Induce time	Ordinary one-way ANOVA
	Emergence time	Ordinary one-way ANOVA
Fig5	Induce time	Ordinary one-way ANOVA
	Emergence time	Ordinary one-way ANOVA
Fig6/7/9	delta wave	two-way ANOVA
	theta wave	two-way ANOVA
	alpha wave	two-way ANOVA
	beta wave	two-way ANOVA
	gamma wave	two-way ANOVA
Fig8	Induce time	Ordinary one-way ANOVA
	Emergence time	Ordinary one-way ANOVA
Fig11	Induce time	Ordinary one-way ANOVA
	Emergence time	Ordinary one-way ANOVA
	quantification of c-fos(+)/TPH2(+) cells	Unpaired t test
	RORR △F/F peak	Unpaired t test

Acknowledgments

The work was supported by the National Natural Science Foundation of China (Grant.NO: 81771403, 81974205); by the Natural Science Foundation of Zhejiang Province (LZ20H090001); by the Program of New Century 131 outstanding young talent plan top-level of Hang Zhou to HHZ

All authors declare no competing interests.

Referrence

1. Taylor NE, *et al.* Optogenetic activation of dopamine neurons in the ventral tegmental area induces reanimation from general anesthesia. *Proc Natl Acad Sci U S A* **113**, 12826-12831 (2016).
2. Brown EN, Lydic R, Schiff ND. General anesthesia, sleep, and coma. *N Engl J Med* **363**, 2638-2650 (2010).
3. Yli-Hankala A, Jantti V, Pyykko I, Lindgren L. Vibration stimulus induced EEG bursts in isoflurane anaesthesia. *Electroencephalogr Clin Neurophysiol* **87**, 215-220 (1993).
4. Land R, Engler G, Kral A, Engel AK. Auditory evoked bursts in mouse visual cortex during isoflurane anesthesia. *PLoS One* **7**, e49855 (2012).
5. Aggarwal A, Brennan C, Shortal B, Contreras D, Kelz MB, Proekt A. Coherence of Visual-Evoked Gamma Oscillations Is Disrupted by Propofol but Preserved Under Equipotent Doses of Isoflurane. *Front Syst Neurosci* **13**, 19 (2019).
6. Hemmings HC, Jr., Akabas MH, Goldstein PA, Trudell JR, Orser BA, Harrison NL. Emerging molecular mechanisms of general anesthetic action. *Trends Pharmacol Sci* **26**, 503-510 (2005).
7. Brown EN, Purdon PL, Van Dort CJ. General anesthesia and altered states of arousal: a systems neuroscience analysis. *Annu Rev Neurosci* **34**, 601-628 (2011).
8. Purdon PL, Sampson A, Pavone KJ, Brown EN. Clinical Electroencephalography

for Anesthesiologists: Part I: Background and Basic Signatures. *Anesthesiology* **123**, 937-960 (2015).
9. Wang TX, *et al.* Activation of Parabrachial Nucleus Glutamatergic Neurons Accelerates Reanimation from Sevoflurane Anesthesia in Mice. *Anesthesiology* **130**, 106-118 (2019).
10. Yin L, *et al.* Optogenetic/Chemogenetic Activation of GABAergic Neurons in the Ventral Tegmental Area Facilitates General Anesthesia via Projections to the Lateral Hypothalamus in Mice. *Front Neural Circuits* **13**, 73 (2019).
11. Vazey EM, Aston-Jones G. Designer receptor manipulations reveal a role of the locus coeruleus noradrenergic system in isoflurane general anesthesia. *Proc Natl Acad Sci U S A* **111**, 3859-3864 (2014).
12. Moore JT, *et al.* Direct activation of sleep-promoting VLPO neurons by volatile anesthetics contributes to anesthetic hypnosis. *Curr Biol* **22**, 2008-2016 (2012).
13. Sah P, Faber ES, Lopez De Armentia M, Power J. The amygdaloid complex: anatomy and physiology. *Physiol Rev* **83**, 803-834 (2003).
14. Wellman LL, Fitzpatrick ME, Hallum OY, Sutton AM, Williams BL, Sanford LD. The basolateral amygdala can mediate the effects of fear memory on sleep independently of fear behavior and the peripheral stress response. *Neurobiol Learn Mem* **137**, 27-35 (2017).
15. Davis M, Walker DL, Miles L, Grillon C. Phasic vs sustained fear in rats and humans: role of the extended amygdala in fear vs anxiety. *Neuropsychopharmacology* **35**, 105-135 (2010).
16. Homma I, Masaoka Y. Breathing rhythms and emotions. *Exp Physiol* **93**, 1011-1021 (2008).
17. Sugita T, *et al.* Breathing is affected by dopamine D2-like receptors in the basolateral amygdala. *Respir Physiol Neurobiol* **209**, 23-27 (2015).
18. Buchanan GF. Timing, sleep, and respiration in health and disease. *Prog Mol Biol Transl Sci* **119**, 191-219 (2013).
19. Buchanan GF, Richerson GB. Central serotonin neurons are required for arousal to CO2. *Proc Natl Acad Sci U S A* **107**, 16354-16359 (2010).
20. McGinty DJ, Harper RM. Dorsal raphe neurons: depression of firing during sleep in cats. *Brain Res* **101**, 569-575 (1976).
21. Saper CB, Fuller PM, Pedersen NP, Lu J, Scammell TE. Sleep state switching. *Neuron* **68**, 1023-1042 (2010).
22. Veasey SC, Fornal CA, Metzler CW, Jacobs BL. Single-unit responses of serotonergic dorsal raphe neurons to specific motor challenges in freely moving cats. *Neuroscience* **79**, 161-169 (1997).
23. Andalman AS, *et al.* Neuronal Dynamics Regulating Brain and Behavioral State Transitions. *Cell* **177**, 970-985 e920 (2019).
24. Ma J, Leung LS. Limbic system participates in mediating the effects of general anesthetics. *Neuropsychopharmacology* **31**, 1177-1192 (2006).
25. Ma J, Shen B, Stewart LS, Herrick IA, Leung LS. The septohippocampal system participates in general anesthesia. *J Neurosci* **22**, RC200 (2002).

26. Long JJ, Shen B, Luo T, Stewart L, McMurran TJ, Leung LS. Pilocarpine model of temporal lobe epilepsy shows enhanced response to general anesthetics. *Exp Neurol* **219**, 308-318 (2009).
27. Bao WW*, et al.* Nucleus accumbens neurons expressing dopamine D1 receptors modulate states of consciousness in sevoflurane anesthesia. *Curr Biol* **31**, 1893-1902 e1895 (2021).
28. Nguyen G, Postnova S. Progress in modelling of brain dynamics during anaesthesia and the role of sleep-wake circuitry. *Biochem Pharmacol* **191**, 114388 (2021).
29. Sutcliffe JG, de Lecea L. The hypocretins: setting the arousal threshold. *Nat Rev Neurosci* **3**, 339-349 (2002).
30. Sakurai T. The neural circuit of orexin (hypocretin): maintaining sleep and wakefulness. *Nat Rev Neurosci* **8**, 171-181 (2007).
31. Peyron C*, et al.* Neurons containing hypocretin (orexin) project to multiple neuronal systems. *J Neurosci* **18**, 9996-10015 (1998).
32. Mashour GA, Pal D, Brown EN. Prefrontal cortex as a key node in arousal circuitry. *Trends Neurosci* **45**, 722-732 (2022).
33. Davis M. The role of the amygdala in fear and anxiety. *Annu Rev Neurosci* **15**, 353-375 (1992).
34. Burlet S, Leger L, Cespuglio R. Nitric oxide and sleep in the rat: a puzzling relationship. *Neuroscience* **92**, 627-639 (1999).
35. Ressler KJ, Nemeroff CB. Role of serotonergic and noradrenergic systems in the pathophysiology of depression and anxiety disorders. *Depress Anxiety* **12 Suppl 1**, 2-19 (2000).
36. Calvo JM, Badillo S, Morales-Ramirez M, Palacios-Salas P. The role of the temporal lobe amygdala in ponto-geniculo-occipital activity and sleep organization in cats. *Brain Res* **403**, 22-30 (1987).
37. Morrison AR, Sanford LD, Ross RJ. The amygdala: a critical modulator of sensory influence on sleep. *Biol Signals Recept* **9**, 283-296 (2000).
38. Portas CM, Thakkar M, Rainnie D, McCarley RW. Microdialysis perfusion of 8-hydroxy-2-(di-n-propylamino)tetralin (8-OH-DPAT) in the dorsal raphe nucleus decreases serotonin release and increases rapid eye movement sleep in the freely moving cat. *J Neurosci* **16**, 2820-2828 (1996).
39. Monti JM, Jantos H. Activation of the serotonin 5-HT3 receptor in the dorsal raphe nucleus suppresses REM sleep in the rat. *Prog Neuropsychopharmacol Biol Psychiatry* **32**, 940-947 (2008).
40. Portas CM, Bjorvatn B, Ursin R. Serotonin and the sleep/wake cycle: special emphasis on microdialysis studies. *Prog Neurobiol* **60**, 13-35 (2000).
41. Rueter LE, Jacobs BL. A microdialysis examination of serotonin release in the rat forebrain induced by behavioral/environmental manipulations. *Brain Res* **739**, 57-69 (1996).
42. Gao J, Zhang JX, Xu TL. Modulation of serotonergic projection from dorsal raphe nucleus to basolateral amygdala on sleep-waking cycle of rats. *Brain Res* **945**, 60-70 (2002).

43. Ungerstedt U. Stereotaxic mapping of the monoamine pathways in the rat brain. *Acta Physiol Scand Suppl* **367**, 1-48 (1971).
44. Ramm P. The locus coeruleus, catecholamines, and REM sleep: a critical review. *Behav Neural Biol* **25**, 415-448 (1979).
45. Aston-Jones G, Bloom FE. Activity of norepinephrine-containing locus coeruleus neurons in behaving rats anticipates fluctuations in the sleep-waking cycle. *J Neurosci* **1**, 876-886 (1981).
45. Shouse MN, Staba RJ, Saquib SF, Farber PR. Monoamines and sleep: microdialysis findings in pons and amygdala. *Brain Res* **860**, 181-189 (2000)